Inhibition of p-glycoprotein does not increase the efficacy of proteasome inhibitors in multiple myeloma cells

Rachel L. Mynott[1] and Craig T. Wallington-Beddoe[1,2,3,4]

[1]College of Medicine and Public Health, Flinders University, Bedford Park SA, 5042, Australia;

[2]Flinders Medical Centre, Bedford Park SA, 5042, Australia;

[3]Centre for Cancer Biology, University of South Australia and SA Pathology, UniSA CRI Building, North Tce, Adelaide SA, 5000, Australia;

[4]Adelaide Medical School, University of Adelaide, Adelaide SA, 5000, Australia;

Corresponding author:

Dr Craig Wallington-Beddoe

Level 4, Flinders Centre for Innovation in Cancer

Flinders University

Bedford Park, SA 5042, Australia

Email: craig.wallingtonbeddoe@flinders.edu.au

Tel: +61 408 080 788;

Abstract

The aim of this study is to determine whether manipulation of the drug transporter P-glycoprotein improves the efficacy of proteasome inhibitors in multiple myeloma. P-glycoprotein is a well-known drug transporter that is associated with chemotherapy resistance in a number of cancers but its role in modulating the efficacy of proteasome inhibitors in multiple myeloma is not well understood. Research has shown that the second generation proteasome inhibitor carfilzomib is a substrate of P-glycoprotein and as such its efficacy may correlate with P-glycoprotein function. In contrast to carfilzomib, research concerning the first-in-class proteasome inhibitor bortezomib is inconsistent. Some researchers have demonstrated that inhibition of P-glycoprotein increases bortezomib cytotoxicity in multiple myeloma cells whereas others have shown no effect. Through the mining of publicly available gene expression microarrays of patient bone marrow, we show that P-glycoprotein gene expression increases with the disease stages leading to multiple myeloma. However, RNA-seq on LP-1 cells treated with bortezomib or carfilzomib demonstrated minimal basal P-glycoprotein expression which did not increase with treatment. Moreover, only one (KMS-18) of nine multiple myeloma cell lines expressed P-glycoprotein, including RPMI-8226 cells that are resistant to bortezomib or carfilzomib. We hypothesised that by inhibiting P-glycoprotein, multiple myeloma cell sensitivity to proteasome inhibitors would increase, thus providing a potential approach to improving responses and reversing resistance to these agents. However, the sensitivity of multiple myeloma cells lines to proteasome inhibition was not enhanced by inhibition of P-glycoprotein with the specific inhibitor tariquidar. In addition, targeting glucosylceramide synthase with eliglustat did not inhibit P-glycoprotein function and also did not improve proteasome inhibitor efficacy except at a high concentration. We conclude that P-glycoprotein

49 is poorly expressed in multiple myeloma cells, its inhibition does not enhance the efficacy of
50 proteasome inhibitors, and it is unlikely to be a useful avenue for further translational research.

51

52 # Introduction

53 Multiple myeloma (MM) is an incurable malignancy of plasma cells (1). The malignant plasma
54 cells usually produce monoclonal immunoglobulin and the disease is characterised by one or
55 more of the four "CRAB" symptoms: high blood calcium, renal insufficiency, anaemia and
56 bone lytic lesions (1). The median age at diagnosis is 69 years, meaning comorbidities and sub-
57 optimal response to chemotherapies make the cancer difficult to treat in many patients (2). MM
58 is currently incurable and if patients do not immediately present with chemotherapy resistance,
59 they will eventually develop such resistance, contributing to a median overall survival of
60 approximately 7 years (1).

61 P-glycoprotein (P-gp) is a well-known drug transporter that has been shown to play a role in
62 drug resistance in a number of solid malignancies where it exports drugs, decreasing their
63 intracellular concentration and thus reducing their efficacy (3, 4). Its relevance in
64 chemotherapy resistance in MM was shown by Dalton *et. al.* where patients previously exposed
65 to chemotherapy had a higher expression of P-gp on their plasma cells compared to newly-
66 diagnosed patients (5). In the context of resistance to proteasome inhibitors, the most important
67 class of novel therapies to treat MM, there have been conflicting reports in the literature. The
68 second generation proteasome inhibitor carfilzomib is a known substrate of P-gp and its
69 efficacy was shown to be enhanced in cancer cells, including MM, when P-gp is inhibited (6-
70 9). In comparison, the efficacy of the first-in-class proteasome inhibitor bortezomib with P-gp
71 inhibition was either improved (10-12) or not affected (6, 13-15) in MM and other human
72 cancer cell lines. Improving the efficacy of proteasome inhibitors in MM and overcoming

resistance to these agents would be very beneficial to improve treatment options for high-P-gp expressing patients.

The activity of P-gp can be inhibited directly, for example with the third-generation P-gp inhibitor tariquidar that blocks the ATPase activity of P-gp (8). However, P-gp can also be indirectly inhibited with research demonstrating that inhibition of the sphingolipid enzyme glucosylceramide synthase (GCS) reduces both gene and protein expression of P-gp (16, 17). GCS converts ceramide to glucosylceramide, the precursor of glycosphingolipids (GSLs) and it has been found that these GSLs upregulate P-gp gene expression via the *cSrc* and β-catenin signalling pathways in cancer cells (16). Eliglustat is a specific and potent inhibitor of GCS, with an EC_{50} in the low nanomolar range, and is used to treat Gaucher's disease (18-20). As an inhibitor of GCS, it reduces glucosylceramide levels in cells and thus GSLs, causing the same reduction in P-gp expression as seen when GCS is either genetically or chemically inhibited by RNA interference or D,L-Threo-1-phenyl-2-palmitoylamino-3-morpholino-1-propanol (PPMP), respectively (21, 22). Therefore, eliglustat can be used to indirectly inhibit P-gp.

Here we report our negative findings, demonstrating P-gp does not appear to be expressed in most MM cell lines, including those resistant to proteasome inhibitors, nor is its expression increased with proteasome inhibitor treatment. Moreover, inhibition of P-gp in MM cell lines does not enhance the efficacy of proteasome inhibitors and may therefore not be a useful avenue for further translational research. Overall, these data support a lack of a role for P-pg in modulating the effects of proteasome inhibitors in MM.

Materials and Methods

95 ## Cell lines

96 RPMI-8226 WT (ATC CCL-155) human MM cell line was obtained from the American Type
97 Culture Collection (Manassas, VA). Resistant RMPI-8226 V10R (bortezomib resistant) and
98 RPMI-8226 C10R (carfilzomib resistant) cell lines were a gift from Professor Stuart Pitson
99 (University of South Australia). LP-1 (ACC 41) human MM cell line was purchased from the
100 Leibniz Institute DSMZ-German Collection of Microorganisms and Cell Cultures GmbH
101 (Braunschweig, Germany). KMS-11 (JCRB1179) human MM cell line was purchased from
102 Cell Bank Australia (Sydney, Australia). MM.1S, MM.1R, NCI-H929 were kindly provided
103 by Prof. Andrew Spencer (Monash University, Vic, Australia) and KMS-18 cells kindly
104 provided by Prof. Junia Melo (SA Pathology, Australia). Cells were cultured in RPMI 1640
105 (Gibco, Waltham, MA) supplemented with 10% foetal bovine serum, 50 units/mL penicillin,
106 0.25 mg/mL streptomycin, 2 mM L-glutamate, 1 mM sodium pyruvate and 15 mM Hepes
107 buffer (all Gibco). Cells were incubated at 37°C in 5% CO_2.

108

109 ## Drugs, reagents and antibodies

110 Bortezomib, carfilzomib and eliglustat were purchased from MedKoo (Morrisville, NC).
111 Tariquidar was purchased from Selleck Chemicals (Houston, TX). Rhodamine 123 (Rho123),
112 propidium iodide (PI) and cOmplete EDTA-free Protease Inhibitor Cocktail were purchased
113 from Sigma Aldrich (St. Louis, MO). Tris UltraPure, hydrochloric acid, sodium chloride,
114 glycerol, β-glycerophosphate and sodium fluoride were purchased from Chem Supply
115 (Adelaide, Australia). FITC Annexin V apoptosis marker, Cat # 556419, AB_2665412 and
116 10X Annexin-V Binding Buffer were purchased from BD Biosciences (San Jose, CA).
117 Precision Plus Protein All Blue and Kaleidoscope Pre-stained Protein Standards molecular

118 weight ladders were purchased from Bio-Rad (Hercules, CA). Vectashield mounting media
119 with 4′,6-diamidino-2-phenylindole (DAPI) was purchased from Vector Labs (Burlingame,
120 CA).

121 FITC Mouse Anti-Human P-glycoprotein (CD243) monoclonal antibody (clone 17F9, Cat #
122 557002, AB_396548) and FITC Mouse IgG2b κ Isotype Control monoclonal antibody (clone
123 27-35, Cat # 555742, AB_396085) were purchased from BD Biosciences. MDR1/ABCB1
124 rabbit monoclonal antibody (clone E1Y7B, Cat # 13342, AB_2631176) was purchased from
125 Cell Signaling (Beverly, MA). Anti-actin mouse monoclonal antibody (clone C4, Cat #
126 MAB1501, AB_2223041) was purchased from Millipore (Burlington, MA). Anti-alpha tubulin
127 mouse antibody loading control (clone DM1A, Cat # ab7291, AB_2241126) was purchased
128 from Abcam (Cambridge, United Kingdom). Pierce Goat Anti-Rabbit IgG (H+L) peroxidase
129 conjugated goat secondary antibody (Cat # 31460, AB_228341) and Pierce Goat Anti-Mouse
130 IgG (H+L) peroxidase conjugated goat secondary antibody (Cat # 31430, AB_228307) were
131 purchased from Invitrogen (Waltham, MA). Cy™5 AffiniPure Donkey Anti-Rabbit IgG
132 (H+L), AB_2340607 and FITC AffiniPure Donkey Anti-Mouse IgG (H+L), AB_2335588
133 polyclonal secondary antibodies were purchased from Jackson Laboratories (Bar Harbor, ME).

134

135 Cell viability by trypan blue

136 Trypan blue (1:2 dilution, Life Technologies, Waltham, MA) was mixed 1:1 with MM cell
137 suspension. 10 µL of this mixture was pipetted onto a haemocytometer slide and cells within
138 the central grid counted. Dead cells were observed as blue whereas live cells were unstained.
139 The concentration of cells was determined by the following equation: n x d x 10,000 = cells/mL
140 where n is the number of cells counted and d is the dilution factor (i.e. 2).

141

142 ## Analysis of DNA microarrays

143 Publicly available gene expression datasets were used to assess P-gp gene expression in
144 CD138-positive bone marrow plasma cells obtained from healthy donors, monoclonal
145 gammopathy of undetermined significance (MGUS), smouldering MM (SMM), newly-
146 diagnosed MM and relapsed MM patients. The following datasets were used: GSE13591
147 (normal, n=5, MGUS, n=11, MM, n=142) (23), E-MTAB-363 (normal, n=5, MGUS, n=5,
148 MM, n=155) (24) and GSE6477 (normal, n=15, MGUS, n=22, smouldering MM, n=24, new
149 MM, n=73, relapsed MM, n=28) (25). Excel (Microsoft Corporation, Redmond, WA) was used
150 to compare differences between two groups using the Student t test ($\log_2$ normally distributed
151 data for GSE13591 and E-MTAB-363 or untransformed data GSE6477).

152

153 ## RNA sequencing and analysis

154 RNA extraction was undertaken using the RNeasy Mini Kit (QIAGEN, Hilden, Germany).
155 Approximately 1 million cells (>80% viable) were treated with proteasome inhibitors for 6 and
156 16 hours before RNA was extracted following instructions provided by the kit. PolyA+
157 enriched RNAseq libraries were multiplexed and sequenced on the Illumina NextSeq 500
158 platform. Raw data, averaging 100 million reads per sample were analysed and quality checked
159 using the FASTQC program (http://www.bioinformatics.babraham.ac.uk/projects/fastqc).
160 Reads were mapped against the human (hg19) reference genomes for LP-1 cells using the
161 STAR spliced alignment algorithm (26) (version2.7.2c with default parameters and -
162 chimSeqmentMin 20, --quantMode GeneCounts) returning an average unique alignment rate
163 of 80%. Differential expression analysis was evaluated from the TMM normalised gene counts
164 using R (version 3.2.3) and edgeR (version 3.3) (27, 28) following protocols as described.

165 Alignments were visualised and interrogated using the Integrative Genomics Viewer v2.3.804.
166 Samples were processed and analysed the Australian Cancer Research Foundation Cancer
167 Genomics Facility (Adelaide, Australia).

168

169 Surface P-glycoprotein expression by flow cytometry

170 Approximately 100,000 – 500,000 MM cells were washed in 1X PBS to pellet. Cell pellets
171 were stained with 2 µL FITC P-gp antibody or matched isotype for 20 minutes in the dark at
172 room temperature. Cells were washed in PBS again to remove unbound antibody. Flow
173 cytometric analysis was undertaken, and data collected from 10,000 events on the CytoFLEX
174 S Flow Cytometer (Beckman Coulter, Brea, CA). CytExpert Software (Beckman Coulter) was
175 used for data collection and analysis.

176

177 Cell viability by flow cytometry

178 Approximately 100,000 – 500,000 MM cells were cultured with and without drugs of interest
179 for up to 72 hours. Cell suspensions were washed in 1X phosphate buffered saline (PBS) and
180 cell pellets stained with 2 µL FITC Annexin-V, 2 µL 1:50 PI and 96 µL 1X Annexin V Binding
181 Buffer for 10 minutes in the dark at room temperature. Cell viability was determined by
182 acquiring 10,000 events using a CytoFLEX S flow cytometer (Beckman Coulter) and analysis
183 of cell viability performed using CytExpert Software (Beckman Coulter). Viable cells are those
184 being dual Annexin-V FITC and PI negative.

185

186 # P-glycoprotein function by Rhodamine 123 efflux

187 Approximately 100,000 – 500,000 MM cells were treated in tissue culture plates with
188 proteasome inhibitors with and without tariquidar or eliglustat. After 22 hours, 200 ng/mL of
189 the cell permeable P-gp substrate Rho123 was added to each well and the plates incubated at
190 37°C, 5% CO_2 for the remaining 2 hours. Cells were then washed twice in 1X PBS and analysed
191 by flow cytometry. Mean fluorescence intensity (MFI) was recorded from 10,000 events on
192 the CytoFLEX S Flow Cytometer (Beckman Coulter). The Rho123 dye is excited by the blue
193 laser (488 nm) and its emission is detected using a 525 nm filter. CytExpert Software (Beckman
194 Coulter) was used for data collection and analysis and data were normalised to unstained,
195 untreated controls.

196

197 # Western blotting

198 3 to 5 million cells were cultured with drugs of interest and then lysed in 10 mM Tris/HCl (pH
199 7.4), 137 mM NaCl containing 10% glycerol, 1% NP40, 10 mM β-glycerophosphate, 2 mM
200 sodium fluoride and cOmplete EDTA-free protease inhibitor cocktail. This remained at 4°C
201 for 10 minutes before centrifugation at 14,000 x g to clarify the lysate. Equal amounts of
202 protein were loaded onto a Mini-PROTEAN TGX Precast Gel (Bio-Rad) and the Trans-Blot
203 Turbo Transfer System was used to transfer protein onto a nitrocellulose membrane (Bio-Rad).
204 Membranes were then blocked in 5% non-fat dairy milk powder in 50 mM Tris (pH 7.4), 154
205 mM NaCl and 1% Tween20 at room temperature for two hours. Primary and secondary
206 antibodies were used as per the manufacturers' instructions and membranes were imaged on
207 the ChemiDoc MP (Bio-Rad) after incubation in Clarity Western ECL Substrate (Bio-Rad).
208 MDR1/ABCB1 and anti-actin primary antibodies were used at a dilution of 1:1000 and 1:5000,

209 respectively, and HRP-conjugated secondary antibodies were used at a dilution of 1:15,000.
210 Image Lab Software (Bio-Rad) was used for densitometric analysis of Western blot images.

211

212 Statistical Analysis

213 Comparisons between two groups were undertaken in Microsoft Excel using the Student t test
214 with a p-value of less than 0.05 considered statistically significant. Synergistic effects of drug
215 combinations were determined using the fractional product method (29) with a value of < -0.1
216 indicating synergy.

217

218 Results

219 Changes in P-gp gene expression with MM disease progression and 220 in response to proteasome inhibitors in MM

221 Publicly available gene expression microarrays were used to analyse P-gp gene expression in
222 CD138-positive purified bone marrow plasma cells. In the three gene expression microarray
223 datasets analysed, newly-diagnosed and relapsed MM patients but not those patients with the
224 precursor conditions monoclonal gammopathy of undetermined significance (MGUS) and
225 smouldering MM (SMM) had higher expression of P-gp when compared to healthy controls
226 (Fig 1). Unlike previous findings (30), there was no statistically significant difference in the
227 expression of P-gp when comparing newly-diagnosed MM patients to patients whose MM had
228 relapsed (Fig 1C), however P-gp appeared to be more highly expressed in MM patients
229 compared to MGUS in two of the datasets (Fig 1A and C).

230

231 **Fig 1. P-gp expression increases with disease progression in MM patients.** Boxplots
232 (median and interquartile range) showing P-gp expression from the GSE13591 (A), E-MTAB-
233 363 (B) and GSE6477 (C) datasets. ns = not statistically significant, * $p < 0.05$. GSE13591
234 (normal, n=5, MGUS, n=11, MM, n=142), E-MTAB-363 (normal, n=5, MGUS, n=5, MM,
235 n=155) and GSE6477 (normal, n=15, MGUS, n=22, smouldering MM, n=24, new MM, n=73,
236 relapsed MM, n=28).

237

238 RNA-seq was undertaken to determine changes gene expression in LP-1 cells treated with 5
239 nM and 10 nM of bortezomib or carfilzomib for 6 hours. Further analysis was undertaken for
240 genes that had a count per million (CPM) of greater than 1 in at least two culture conditions.
241 Consequently, the data showed that P-gp was minimally expressed in this cell line (CPM < 1
242 for the control and proteasome inhibitor treatment groups) and so further normalisation and
243 analysis was not undertaken for this gene.

244

245 Basal P-gp protein expression in MM cell lines

246 Surface P-gp expression was analysed by flow cytometry. When compared to isotype, there
247 appeared to be no P-gp expression on the surface of any of the human MM cell lines tested (Fig
248 2A). However, analysis of total cell P-gp by Western blot indicated that KMS-18 cells did
249 express P-gp, whilst the other 8 MM cell lines examined, including the RPMI-8226
250 bortezomib/carfilzomib resistant cells, did not (Fig 2B). Due to the lack of P-gp in all MM cell
251 lines aside from KMS-18, the latter cell line was used for most subsequent experiments
252 exploring P-gp expression and function.

253

254 **Fig 2. Basal P-gp in MM cell lines.** A) Cell surface P-gp MFI of MM cell lines relative to
255 isotype control. Data are mean ± standard deviation of three independent experiments (two
256 independent experiments for RPMI-8226 WT, RPMI-8226 V10R, MM.1S, MM.1R and KMS-
257 11). B) Western blot probed for total cell P-gp (170 kDa) in human MM cell lines. β-actin used
258 as loading control. RPMI WT = RPMI-8226 WT, C10R = RPMI-8226 C10R, V10R = RPMI-
259 8226 V10R and H929 = NCI-H929.

260

261 Changes in P-gp expression, function and cell viability in response 262 to proteasome, P-gp and GCS inhibition

263 Proteasome inhibitors and changes in P-gp

264 LP-1 and KMS-18 MM cells cultured with bortezomib or carfilzomib for 24 hours did not
265 appear to result in a clear increase in surface P-gp expression by flow cytometry (Fig 3A and
266 C). Bortezomib appeared to have a greater cytotoxic effect than carfilzomib in both LP-1 and
267 KMS-18 cells despite carfilzomib being shown to be more effective than bortezomib in MM
268 patients (Fig 3B and D) (31). Despite not causing an increase in surface P-gp in KMS-18 cells,
269 bortezomib did result in total P-gp expression increasing after a 16-hour treatment (Fig 3E).
270 Carfilzomib caused a more gradual increase in total P-gp expression, requiring a higher
271 concentration to double the level of P-gp expression compared to the control culture (Fig 3F).

272

273 **Fig 3. P-gp surface and total expression, and cell viability for MM cell lines treated with**
274 **proteasome inhibitors.** KMS-18 cells were treated with bortezomib or carfilzomib for 24

275 hours and flow cytometric analysis was undertaken to determine surface P-gp expression (A)
276 and cell viability (B). LP-1 cells were treated with bortezomib or carfilzomib for 24 hours and
277 flow cytometric analysis was undertaken to determine surface P-gp expression (C) and cell
278 viability (D). Viability is represented as fold change relative to untreated control cultures.
279 KMS-18: Bortezomib data are mean ± standard deviation of duplicates from four biological
280 replicates for 0, 4 and 10 nM treatments and two technical replicates for the remaining
281 conditions. Carfilzomib data are mean ± standard deviation of duplicates of four biological
282 replicates for 0, 10 and 20 nM treatments and duplicates of two biological replicates for the
283 remaining conditions. LP-1: Bortezomib data are mean ± standard deviation of duplicates from
284 two biological replicates for 0, 4 and 10 nM treatments and two technical replicates for the
285 remaining treatments. Carfilzomib data are mean ± standard deviation of two technical
286 replicates. KMS-18 cells were treated with bortezomib (E) or carfilzomib (F) for 16 hours and
287 total P-gp expression was determined by Western blot. Associated densitometric analyses are
288 displayed below each blot with P-gp band intensity relative to respective β-actin loading
289 control.

290

291 **Inhibiting P-gp directly with tariquidar**

292 Bortezomib alone caused an increase in total P-gp expression in KMS-18 cells which was not
293 greatly altered by the addition of 1 μM tariquidar (Fig 4A and B), a concentration shown to
294 effectively inhibit P-gp in cancer cells (32). The combination of bortezomib with tariquidar did
295 not appear to cause a statistically significant increase in surface P-gp expression (Fig 4C).
296 When KMS-18 cells were cultured with bortezomib alone, Rho123 MFI decreased with
297 increasing concentrations of the drug, likely due to efflux of Rho123 from the cell. The addition
298 of tariquidar inhibited the function of P-gp as expected, causing an accumulation of Rho123 as

299 seen by Rho123 MFI remaining constant with increasing concentrations of bortezomib (Fig
300 4D). The addition of tariquidar did not appear to further sensitise cells to the cytotoxic effects
301 of bortezomib, as neither an additive nor synergistic increase in cell death was seen in KMS-
302 18 cells treated with the combination of the two drugs (Fig 4E).

303

304 **Fig 4. Tariquidar functionally inhibits P-gp but does not synergise with bortezomib**. A)
305 Western blot for KMS-18 cells treated with bortezomib and 0 or 1 μM tariquidar for 16 hours.
306 B) Densitometric analysis of the Western blot displayed in (A), P-gp band intensity relative to
307 respective β-actin loading control. KMS-18 cells were treated with bortezomib and 0, 1 or 5
308 μM tariquidar for 24 hours. Surface P-gp expression relative to isotype (C), Rho123 MFI
309 normalised to unstained and relative to untreated (first data point of blue line) controls (D) and
310 viability relative to untreated control (E) were analysed by flow cytometry. Flow cytometry
311 data are mean ± standard deviation from two independent experiments. ** $p < 0.01$.

312

313 Carfilzomib alone did not appear to greatly change total P-gp expression in KMS-18 cells at
314 the concentrations tested, however, the addition of 1 μM tariquidar caused a slight decrease
315 (Fig 5A and B). On the cell surface, 5 μM tariquidar resulted in a small increase in P-gp
316 expression when combined with 20 nM carfilzomib (Fig 5C). When KMS-18 cells were
317 cultured with carfilzomib alone, the Rho123 MFI decreased with increasing concentrations of
318 the drug, suggesting an increase in efflux of the dye. The treatments combining carfilzomib
319 with tariquidar resulted in a much smaller decrease in Rho123 MFI, suggesting the addition of
320 tariquidar causes an accumulation of dye in the cells when compared to carfilzomib alone,
321 consistent with functional inhibition of P-gp by tariquidar (Fig 5D). As with bortezomib, the
322 addition of tariquidar did not appear to further sensitise cells to the cytotoxic effects of

323 carfilzomib, as neither an additive nor synergistic reduction in cell viability was observed in
324 cells treated with the combination of the two drugs (Fig 5E).

325

326 **Fig 5. Tariquidar functionally inhibits P-gp but does not synergise with carfilzomib**. A)
327 Western blot for KMS-18 cells treated with carfilzomib and 0 or 1 μM tariquidar for 16 hours.
328 B) Densitometric analysis of Western blot displayed in (A), P-gp band intensity relative to
329 respective β-actin loading control. KMS-18 cells were treated with carfilzomib and 0, 1 or 5
330 μM tariquidar for 24 hours. Surface P-gp expression relative to isotype (C), Rho123 MFI
331 normalised to unstained and relative to untreated (first data point of blue line) controls (D) and
332 viability relative to untreated (E) were analysed by flow cytometry. Flow cytometry data are
333 mean ± standard deviation of two independent experiments. ** $p < 0.01$.

334

335 Inhibiting glucosylceramide synthase

336 The potent and specific GCS inhibitor eliglustat alone did not alter total P-gp expression in
337 KMS-18 cells, however, 30 μM eliglustat, the highest concentration examined, augmented the
338 increase in P-gp induced by bortezomib (Fig 6A and B). Intriguingly, this combination did not
339 result in increased surface P-gp expression (Fig 6C). P-gp function as indicated by Rho123 cell
340 efflux did not appear to be affected by eliglustat treatment as the MFI of the dye decreased to
341 the same extent when comparing bortezomib alone to bortezomib plus eliglustat treatment (Fig
342 6D). These data agree with previous findings demonstrating GCS downregulation by antisense
343 transfection did not influence Rho123 efflux in an adriamycin-resistant breast adenocarcinoma
344 cell line with high P-gp expression (33). The addition of eliglustat did, however, further
345 sensitise KMS-18 cells to bortezomib, as a synergistic reduction in cell viability was seen with
346 bortezomib and 30 μM eliglustat (Fig 6E) (fractional product -0.314 and -0.216 for 4 nM and

347 10 nM bortezomib, respectively), despite eliglustat being shown to inhibit GCS at
348 concentrations in the low nanomolar range (19, 20).

349

350 **Fig 6. Eliglustat does not inhibit P-gp but synergises with bortezomib**. A) Western blot of
351 KMS-18 cells treated with bortezomib and 0, 40 nM or 30 μM eliglustat for 16 hours. B)
352 Densitometric analysis of the Western blot displayed in (A), P-gp band intensity relative to
353 respective β-actin loading control. KMS-18 cells were treated with bortezomib and 0, 40 nM
354 or 30 μM eliglustat for 24 hours. Surface P-gp expression relative to isotype (C), Rho123 MFI
355 normalised to unstained and relative to untreated (first data point of blue line) controls (D) and
356 viability relative to untreated control (E) were analysed by flow cytometry. Flow cytometry
357 data are mean ± standard deviation of duplicate measurements and are representative of two
358 independent experiments. ** $p < 0.01$.

359

360 The addition of 30 μM eliglustat to carfilzomib treatment also produced an increase in total P-
361 gp (Fig 7A and B), and to a lesser extent surface P-gp (Fig 7C). Rho123 efflux and thus P-gp
362 function did not appear to be affected by eliglustat treatment as the MFI of the dye decreased
363 to the same extent when comparing carfilzomib alone to carfilzomib plus eliglustat treatment
364 (Fig 7D). This correlates with the bortezomib and eliglustat data (Fig 6), suggesting inhibition
365 of GCS by eliglustat does not inhibit P-gp function. The addition of eliglustat did, however,
366 appear to further sensitise the cells to carfilzomib treatment, as a synergistic reduction in cell
367 viability was seen with carfilzomib and 30 μM eliglustat (Fig 7E) (fractional product -0.446
368 and -0.390 for 10 nM and 20 nM carfilzomib, respectively).

369

370 **Fig 7. Eliglustat does not inhibit P-gp but synergises with carfilzomib**. A) Western blot for
371 KMS-18 cells treated with carfilzomib and 0, 40 nM or 30 μM eliglustat for 16 hours. B)
372 Densitometric analysis of the Western blot displayed in (A), P-gp band intensity relative to
373 respective β-actin loading control. KMS-18 cells were treated with carfilzomib and 0, 40 nM
374 or 30 μM eliglustat for 24 hours. Surface P-gp expression relative to isotype (C), Rho123 MFI
375 normalised to unstained and relative to untreated (first data point of blue line) controls (D) and
376 viability relative to untreated control (E) were analysed by flow cytometry. Flow cytometry
377 data are mean ± standard deviation of duplicate measurements and are representative of two
378 independent experiments. *, $p < 0.05$, ** $p < 0.01$.

379

380 As a comparison to KMS-18 cells, LP-1 cells do not express P-gp and unlike KMS-18 cells,
381 bortezomib treatment does not upregulate P-gp protein expression by Western blot (Fig 8A).
382 Rho123 MFI remains constant with bortezomib alone or in combination with eliglustat,
383 suggesting the dye is being retained in the cell, likely due to the absence of P-gp (Fig 8B).
384 However, LP-1 cells appear to be more sensitive to eliglustat treatment alone at 30 μM
385 compared to KMS-18, as a 20% reduction in viability in LP-1 cells was observed (Fig 8C),
386 compared to no significant change in viability in KMS-18 cells (Figs 6E and 7E). Moreover, a
387 synergistic reduction in cell viability with the combination of drugs was not evident as was
388 seen in KMS-18 cells which express P-gp (Fig 8C).

389

390 **Fig 8. LP-1 cells do not express P-glycoprotein**. A) Western blot for LP-1 cells treated with
391 bortezomib and 0, 40 nM or 30 μM eliglustat for 16 hours, β-actin used as a loading control.
392 LP-1 cells were treated with bortezomib and 0, 40 nM or 30 μM eliglustat for 24 hours and the
393 Rho123 MFI normalised to unstained and relative to untreated (first data point of blue line)

394 controls (B) and viability relative to untreated control (C) were analysed by flow cytometry.
395 Flow cytometry data are mean ± standard deviation of two technical replicates.

396

397 Discussion

398 Despite the most well-known and researched function of P-gp being that of drug efflux when
399 located on the plasma membrane, it has also been shown to play a role in drug resistance when
400 situated in intracellular organelles such as lysosomes, mitochondria and nuclei (34-36). This
401 may explain the strong presence of P-gp in KMS-18 whole cell lysates by Western blot whilst
402 flow cytometric analysis demonstrated that it was not expressed to a great extent on the cell
403 surface. Despite these cells not expressing high levels of P-gp on the plasma membrane before
404 or after proteasome inhibitor treatment, they did show a decrease in Rho123 fluorescence
405 which is indicative of heightened P-gp function. Whilst this may be because the low level of
406 P-gp already on the surface is sufficient to pump out the dye, it could also be related to the
407 greater whole cell P-gp expression observed after proteasome inhibitor treatment and
408 catabolism of the dye in intracellular compartments such as lysosomes on which P-gp is present
409 (37). It has also been suggested that P-gp is regulated by post-translational modifications such
410 phosphorylation and assessing these modifications may be useful to determine whether they
411 have an effect on the activity of P-gp without changing the level of protein on the surface (38).

412 The other eight human MM cell lines tested, including bortezomib/carfilzomib resistant RPMI-
413 8226 cells, did not express P-gp on the cell surface or in whole cell lysates. Furthermore, its
414 expression was not induced by proteasome inhibition in LP-1 or H929 cells, indicated by a lack
415 of protein band at 170 kDa (H929 Western blot displayed in Fig S1). The Rho123 efflux studies
416 confirm this as the dye was retained in LP-1 cells treated with bortezomib, a response similar
417 to that observed for KMS-18 cells when P-gp was inhibited (Figs 4 and 5). Our RNA-seq data

418 also support this, with minimal P-gp gene expression found in LP-1 cells treated with
419 proteasome inhibitors, therefore this cell line and the remaining 7 MM cell lines were not used
420 in further P-gp experiments. These data support the findings that most MM cell lines have low
421 P-gp expression, making it difficult to test its contribution to proteasome inhibitor cellular
422 efflux (12). Unfortunately, the doxorubicin resistant MM cell line (RPMI-8226/Dox40) that
423 has been shown to have high P-gp expression could not be obtained and would be a useful
424 positive control for experiments assessing P-gp expression and function (11, 39).

425 Tariquidar is a functional inhibitor of P-gp, blocking its ATPase activity, and as expected it did
426 not directly affect P-gp expression (8). Tariquidar was shown to effectively inhibit P-gp in MM
427 cells at a concentration of 5 μM (8) and 1 μM in other cancers (32), so these concentrations
428 were chosen for further investigation in KMS-18 MM cells. Both 1 μM and 5 μM tariquidar
429 resulted in a decrease in P-gp function when combined with bortezomib, as shown by an
430 accumulation of Rho123 in the KMS-18 cells. Conversely, bortezomib treatment alone resulted
431 in an increase in P-gp activity in these cells. These data contradict a previous report where after
432 24 hours in culture with bortezomib, RPMI-8226/Dox40 MM cells had a reduction in P-gp
433 activity shown by an accumulation of Rho123 in the cells and a reduction of P-gp protein
434 expression by Western blot (11). Despite tariquidar inhibiting P-gp, it did not further sensitise
435 the cells to bortezomib. This is consistent with previous studies showing bortezomib is not a
436 substrate of P-gp (6, 13-15), however, contradicts research that showed inhibition of P-gp does
437 improve the efficacy of bortezomib in MM cell lines (11, 12).

438 Carfilzomib requires higher concentrations compared to bortezomib to produce an increase in
439 total cell P-gp expression by Western blot. Similar to bortezomib, it does not induce P-gp
440 expression on the cell surface by flow cytometry, however, Rho123 fluorescence and thus P-
441 gp function does increase with increasing concentrations of carfilzomib. The combination of 5
442 μM tariquidar with 20 nM carfilzomib did cause a very small increase in surface P-gp which

443 may be to compensate for P-gp inhibition. Despite the literature suggesting that carfilzomib is
444 a substrate of P-gp (6-9), inhibition of P-gp by tariquidar did not further sensitise KMS-18 cells
445 to carfilzomib treatment. Taken together, these data demonstrate that P-gp inhibition does not
446 improve the efficacy of bortezomib or carfilzomib, suggesting drug efflux by P-gp may not be
447 a mechanism underpinning proteasome inhibitor resistance in MM.

448 Despite another research group (8) showing 5 μM tariquidar was sufficient to further sensitise
449 MM.1S MM cells to 5 nM bortezomib and carfilzomib, this concentration of tariquidar did not
450 enhance proteasome inhibitor induced cell death in KMS-18 cells. Using a higher tariquidar
451 concentration and longer incubation period may be valuable to confirm these results in KMS-
452 18 MM cells. It is important to note that whilst no changes in cell viability were observed,
453 changes in cell cycle and proliferation were not examined. It is entirely possible that the
454 combination of tariquidar with a proteasome inhibitor mediates changes in cell proliferation
455 rather than cell viability and this could be assessed in the future.

456 A link between glucosylceramides and P-gp has been established but is not well understood.
457 Genetic or chemical inhibition of GCS which converts ceramide to glucosylceramide has been
458 shown to downregulate P-gp expression (17) and so these findings led us to use the potent and
459 specific GCS inhibitor eliglustat as a way to indirectly inhibit P-gp. Interestingly, eliglustat did
460 not functionally inhibit P-gp as there were no significant changes in Rho123 fluorescence
461 before or after combining bortezomib/carfilzomib with eliglustat, thereby not supporting the
462 hypothesis that GCS inhibition downregulates P-gp expression and/or activity, at least in MM
463 cells. Eliglustat did, however, produce synergistic cell death when combined with bortezomib
464 and carfilzomib but only at a high concentration (30 μM) despite only needing a concentration
465 in the low nanomolar range to inhibit GCS enzymatic activity (19, 20). This high concentration
466 of eliglustat and the fact that it did not inhibit the function of P-gp suggests off target effects
467 may be causing this synergistic reduction in cell viability. One research group showed that

468 downregulation of GCS by siRNA-mediated knockdown slowed the clearance of ceramide
469 which is pro-apoptotic, and so an accumulation of ceramide may be contributing to the increase
470 in cell death observed in cells treated with 30 μM eliglustat and a proteasome inhibitor (17).
471 Such a high concentration of eliglustat is likely not clinically achievable so these data suggest
472 eliglustat may not be an effective drug to further sensitise MM cells to proteasome inhibition.

473 P-gp plays a role in chemotherapy resistance in a number of cancers, however its role in
474 contributing to proteasome inhibitor efficacy in MM is less well studied with conflicting reports
475 in the literature. Our data presented herein suggests that P-gp is poorly expressed in MM cells,
476 including those resistant to proteasome inhibitors, and that inhibition of P-gp does not enhance
477 proteasome inhibitor efficacy. Thus, a strategy to either increase the efficacy of proteasome
478 inhibitors or reverse resistance to these agents in MM via inhibition of P-gp may not be worthy
479 of further exploration.

480

481 # Acknowledgements

482 CWB was supported by a Sylvia and Charles Viertel Foundation Clinical Investigator Award
483 and a Royal Australasian College of Physicians Servier 'Barry Young' Research Establishment
484 Fellowship.

485

486 # References

487 1. Rajkumar SV, Kumar S. Multiple Myeloma: Diagnosis and Treatment. Mayo Clinic
488 Proceedings. 2016;91(1):101-19.
489 2. Wallington-Beddoe CT, Sobieraj-Teague M, Kuss BJ, Pitson SM. Resistance to
490 proteasome inhibitors and other targeted therapies in myeloma. British Journal of
491 Haematology. 2018;182(1):11-28.

492 3. Abraham J, Salama NN, Azab AK. The role of P-glycoprotein in drug resistance in
493 multiple myeloma. Leukemia & Lymphoma. 2015;56(1):26-33.
494 4. Nigam SK. What do drug transporters really do? Nat Rev Drug Discov. 2015;14(1):29-
495 44.
496 5. Dalton WS. Detection of multidrug resistance gene expression in multiple myeloma.
497 Leukemia. 1997;11(7):1166-9.
498 6. Verbrugge SE, Assaraf YG, Dijkmans BAC, Scheffer GL, Al M, den Uyl D, et al.
499 Inactivating PSMB5 Mutations and P-Glycoprotein (Multidrug Resistance-Associated
500 Protein/ATP-Binding Cassette B1) Mediate Resistance to Proteasome Inhibitors: Ex Vivo
501 Efficacy of (Immuno)Proteasome Inhibitors in Mononuclear Blood Cells from Patients with
502 Rheumatoid Arthritis. Journal of Pharmacology and Experimental Therapeutics.
503 2012;341(1):174-82.
504 7. Besse A, Stolze SC, Rasche L, Weinhold N, Morgan GJ, Kraus M, et al. Carfilzomib
505 resistance due to ABCB1/MDR1 overexpression is overcome by nelfinavir and lopinavir in
506 multiple myeloma. Leukemia. 2018;32:391.
507 8. Muz B, Kusdono HD, Azab F, de la Puente P, Federico C, Fiala M, et al. Tariquidar
508 sensitizes multiple myeloma cells to proteasome inhibitors via reduction of hypoxia-induced
509 P-gp-mediated drug resistance. Leukemia & Lymphoma. 2017;58(12):2916-25.
510 9. Ao L, Wu Y, Kim D, Jang ER, Kim K, Lee D-M, et al. Development of peptide-based
511 reversing agents for p-glycoprotein-mediated resistance to carfilzomib. Mol Pharm.
512 2012;9(8):2197-205.
513 10. Rumpold H, Salvador C, Wolf AM, Tilg H, Gastl G, Wolf D. Knockdown of PgP
514 resensitizes leukemic cells to proteasome inhibitors. Biochemical and Biophysical Research
515 Communications. 2007;361(2):549-54.
516 11. O'Connor R, Ooi MG, Meiller J, Jakubikova J, Klippel S, Delmore J, et al. The
517 interaction of bortezomib with multidrug transporters: implications for therapeutic applications
518 in advanced multiple myeloma and other neoplasias. Cancer chemotherapy and pharmacology.
519 2013;71(5):1357-68.
520 12. Clemens J, Seckinger A, Hose D, Theile D, Longo M, Haefeli WE, et al. Cellular uptake
521 kinetics of bortezomib in relation to efficacy in myeloma cells and the influence of drug
522 transporters. Cancer chemotherapy and pharmacology. 2015;75(2):281-91.
523 13. Lu S, Wang J. The resistance mechanisms of proteasome inhibitor bortezomib.
524 Biomarker Research. 2013;1.
525 14. Minderman H, Zhou Y, O'Loughlin KL, Baer MR. Bortezomib activity and in vitro
526 interactions with anthracyclines and cytarabine in acute myeloid leukemia cells are
527 independent of multidrug resistance mechanisms and p53 status. Cancer chemotherapy and
528 pharmacology. 2007;60(2):245-55.
529 15. de Wilt LHAM, Jansen G, Assaraf YG, van Meerloo J, Cloos J, Schimmer AD, et al.
530 Proteasome-based mechanisms of intrinsic and acquired bortezomib resistance in non-small
531 cell lung cancer. Biochemical Pharmacology. 2012;83(2):207-17.
532 16. Liu Y-Y, Gupta V, Patwardhan GA, Bhinge K, Zhao Y, Bao J, et al. Glucosylceramide
533 synthase upregulates MDR1 expression in the regulation of cancer drug resistance through cSrc
534 and β-catenin signaling. Molecular Cancer. 2010;9(1):145.
535 17. Gouazé V, Liu Y-Y, Prickett CS, Yu JY, Giuliano AE, Cabot MC. Glucosylceramide
536 Synthase Blockade Down-Regulates P-Glycoprotein and Resensitizes Multidrug-Resistant
537 Breast Cancer Cells to Anticancer Drugs. Cancer Research. 2005;65(9):3861-7.
538 18. Scott LJ. Eliglustat: A Review in Gaucher Disease Type 1. Drugs. 2015;75(14):1669-
539 78.

19. McEachern KA, Fung J, Komarnitsky S, Siegel CS, Chuang W-L, Hutto E, et al. A specific and potent inhibitor of glucosylceramide synthase for substrate inhibition therapy of Gaucher disease. Molecular Genetics and Metabolism. 2007;91(3):259-67.
20. Shayman JA. Eliglustat tartrate, a prototypic glucosylceramide synthase inhibitor. Expert Review of Endocrinology & Metabolism. 2013;8(6):491-504.
21. Roh J-L, Kim EH, Park JY, Kim JW. Inhibition of Glucosylceramide Synthase Sensitizes Head and Neck Cancer to Cisplatin. Molecular Cancer Therapeutics. 2015;14(8):1907-15.
22. Xie P, Shen Y-F, Shi Y-P, Ge S-M, Gu Z-H, Wang J, et al. Overexpression of glucosylceramide synthase in associated with multidrug resistance of leukemia cells. Leukemia Research. 2008;32(3):475-80.
23. Agnelli L, Mosca L, Fabris S, Lionetti M, Andronache A, Kwee I, et al. A SNP microarray and FISH-based procedure to detect allelic imbalances in multiple myeloma: an integrated genomics approach reveals a wide gene dosage effect. Genes, chromosomes & cancer. 2009;48(7):603-14.
24. Rème T, Hose D, Theillet C, Klein B. Modeling risk stratification in human cancer. Bioinformatics. 2013;29(9):1149-57.
25. Chng WJ, Kumar S, Vanwier S, Ahmann G, Price-Troska T, Henderson K, et al. Molecular dissection of hyperdiploid multiple myeloma by gene expression profiling. Cancer Res. 2007;67(7):2982-9.
26. Dobin A, Davis CA, Schlesinger F, Drenkow J, Zaleski C, Jha S, et al. STAR: ultrafast universal RNA-seq aligner. Bioinformatics. 2012;29(1):15-21.
27. Robinson MD, McCarthy DJ, Smyth GK. edgeR: a Bioconductor package for differential expression analysis of digital gene expression data. Bioinformatics. 2010;26(1):139-40.
28. Lun AT, Chen Y, Smyth GK. It's DE-licious: A Recipe for Differential Expression Analyses of RNA-seq Experiments Using Quasi-Likelihood Methods in edgeR. Methods Mol Biol. 2016;1418:391-416.
29. Webb JL. Effect of more than one inhibitor. Enzyme and metabolic Inhibitors. 1963;1:66-79,488-512.
30. Grogan T, Spier C, Salmon S, Matzner M, Rybski J, Weinstein R, et al. P-glycoprotein expression in human plasma cell myeloma: correlation with prior chemotherapy. Blood. 1993;81(2):490-5.
31. Dimopoulos M, Siegel D, White DJ, Boccia R, Iskander KS, Yang Z, et al. Carfilzomib vs bortezomib in patients with multiple myeloma and renal failure: a subgroup analysis of ENDEAVOR. Blood. 2019;133(2):147.
32. Weidner LD, Fung KL, Kannan P, Moen JK, Kumar JS, Mulder J, et al. Tariquidar Is an Inhibitor and Not a Substrate of Human and Mouse P-glycoprotein. Drug Metab Dispos. 2016;44(2):275-82.
33. Liu Y-Y, Han T-Y, Giuliano AE, Cabot MC. Ceramide glycosylation potentiates cellular multidrug resistance. The FASEB Journal. 2001;15(3):719-30.
34. Yamagishi T, Sahni S, Sharp DM, Arvind A, Jansson PJ, Richardson DR. P-glycoprotein mediates drug resistance via a novel mechanism involving lysosomal sequestration. J Biol Chem. 2013;288(44):31761-71.
35. Solazzo M, Fantappie O, Lasagna N, Sassoli C, Nosi D, Mazzanti R. P-gp localization in mitochondria and its functional characterization in multiple drug-resistant cell lines. Experimental cell research. 2006;312(20):4070-8.
36. Baldini N, Scotlandi K, Serra M, Shikita T, Zini N, Ognibene A, et al. Nuclear immunolocalization of P-glycoprotein in multidrug-resistant cell lines showing similar mechanisms of doxorubicin distribution. European journal of cell biology. 1995;68(3):226-39.

590 37. Forster S, Thumser AE, Hood SR, Plant N. Characterization of Rhodamine-123 as a
591 Tracer Dye for Use In In vitro Drug Transport Assays. PLOS ONE. 2012;7(3):e33253.
592 38. Callaghan R, Luk F, Bebawy M. Inhibition of the Multidrug Resistance P-
593 Glycoprotein: Time for a Change of Strategy? Drug Metabolism and Disposition.
594 2014;42(4):623.
595 39. Hawley TS, Riz I, Yang W, Wakabayashi Y, DePalma L, Chang Y-T, et al.
596 Identification of an ABCB1 (P-glycoprotein)-positive carfilzomib-resistant myeloma
597 subpopulation by the pluripotent stem cell fluorescent dye CDy1. American Journal of
598 Hematology. 2013;88(4):265-72.

599

600 Supporting Information

601 **Fig S1. H929 MM cells do not express P-gp.** Western blot probed for P-gp (170 kDa) in H929

602 cells treated with bortezomib ± tariquidar for 16 hours, showing H929 cells do not express P-

603 gp.

604 **Fig S2. Raw Western blot images.**

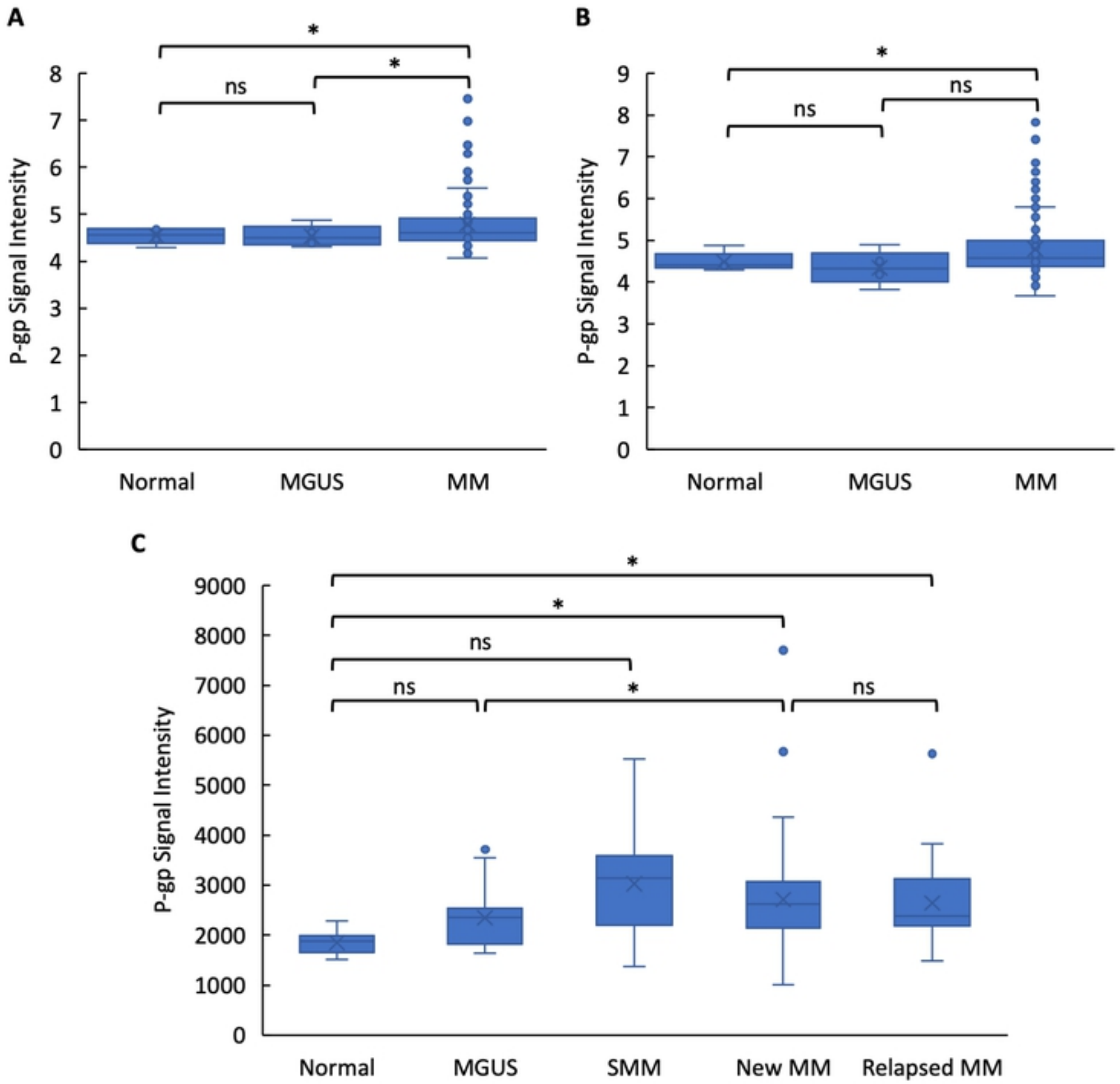
A
P-gp Signal Intensity
0
1
2
3
4
5
6
7
8
ns
*
*
Normal
MGUS
MM
B
P-gp Signal Intensity
0
1
2
3
4
5
6
7
8
9
ns
ns
*
Normal
MGUS
MM
C
P-gp Signal Intensity
0
1000
2000
3000
4000
5000
6000
7000
8000
9000
ns
ns
*
*
ns
*
Normal
MGUS
SMM
New MM
Relapsed MM

Figure 1

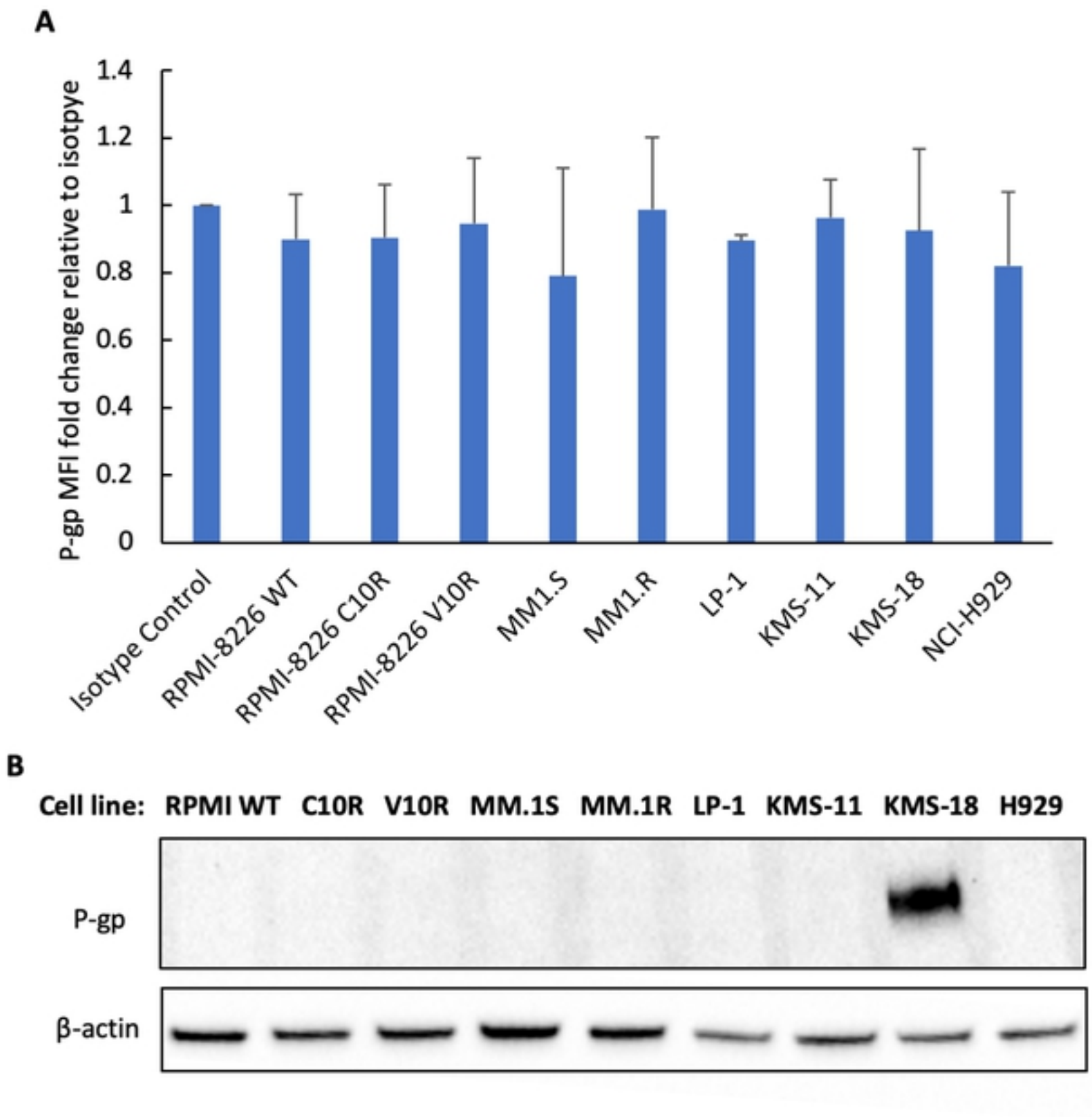
A
P-gp MFI fold change relative to isotpye
1.4
1.2
1
0.8
0.6
0.4
0.2
0
Isotype Control
RPMI-8226 WT
RPMI-8226 C10R
RPMI-8226 V10R
MM1.S
MM1.R
LP-1
KMS-11
KMS-18
NCI-H929
B
Cell line: RPMI WT C10R V10R MM.1S MM.1R LP-1 KMS-11 KMS-18 H929
P-gp
β-actin

Figure 2

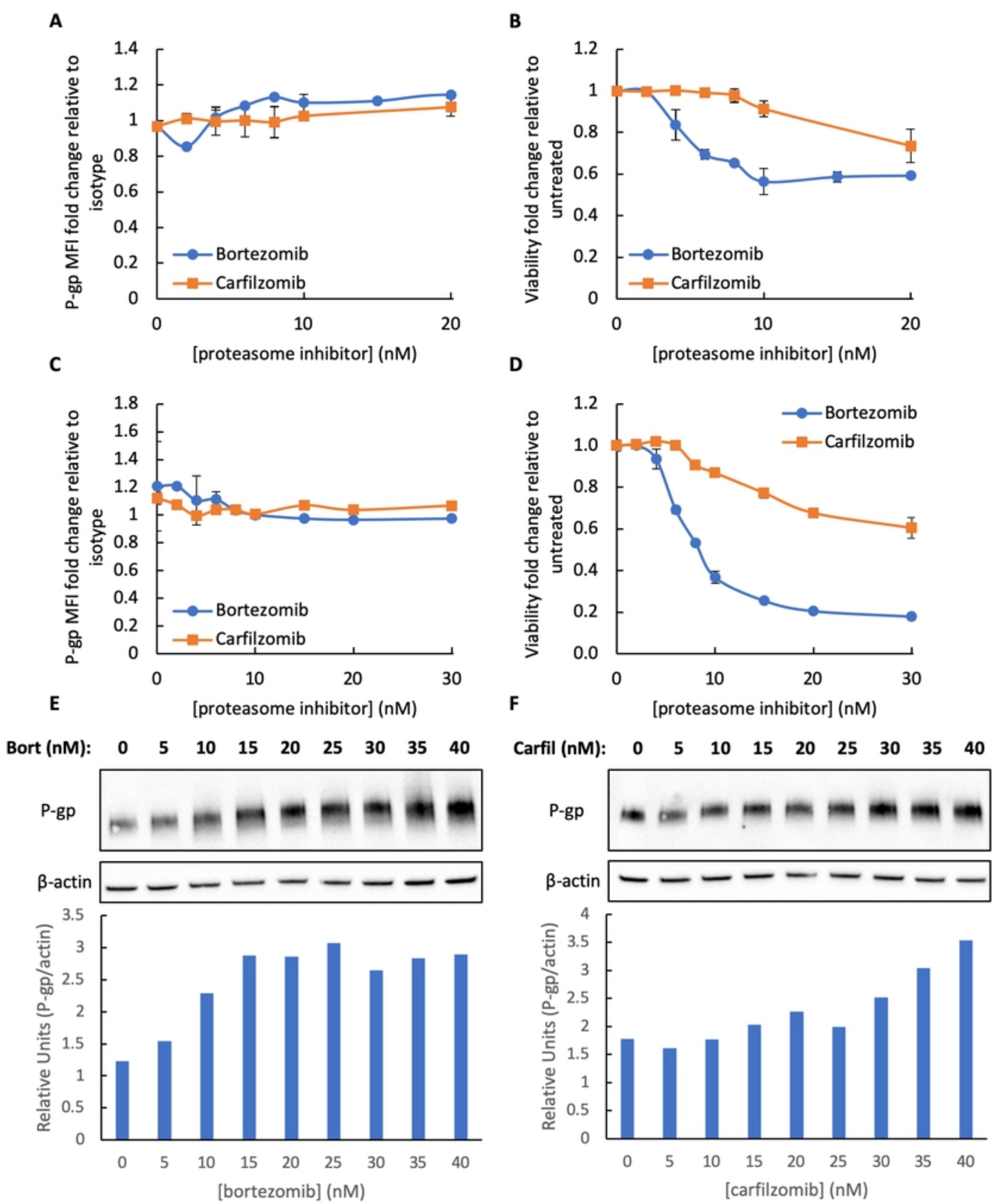
A
P-gp MFI fold change relative to isotype
Bortezomib
Carfilzomib
[proteasome inhibitor] (nM)
B
Viability fold change relative to untreated
Bortezomib
Carfilzomib
[proteasome inhibitor] (nM)
C
P-gp MFI fold change relative to isotype
Bortezomib
Carfilzomib
[proteasome inhibitor] (nM)
D
Viability fold change relative to untreated
Bortezomib
Carfilzomib
[proteasome inhibitor] (nM)
E
Bort (nM): 0 5 10 15 20 25 30 35 40
P-gp
β-actin
Relative Units (P-gp/actin)
[bortezomib] (nM)
F
Carfil (nM): 0 5 10 15 20 25 30 35 40
P-gp
β-actin
Relative Units (P-gp/actin)
[carfilzomib] (nM)

Figure 3

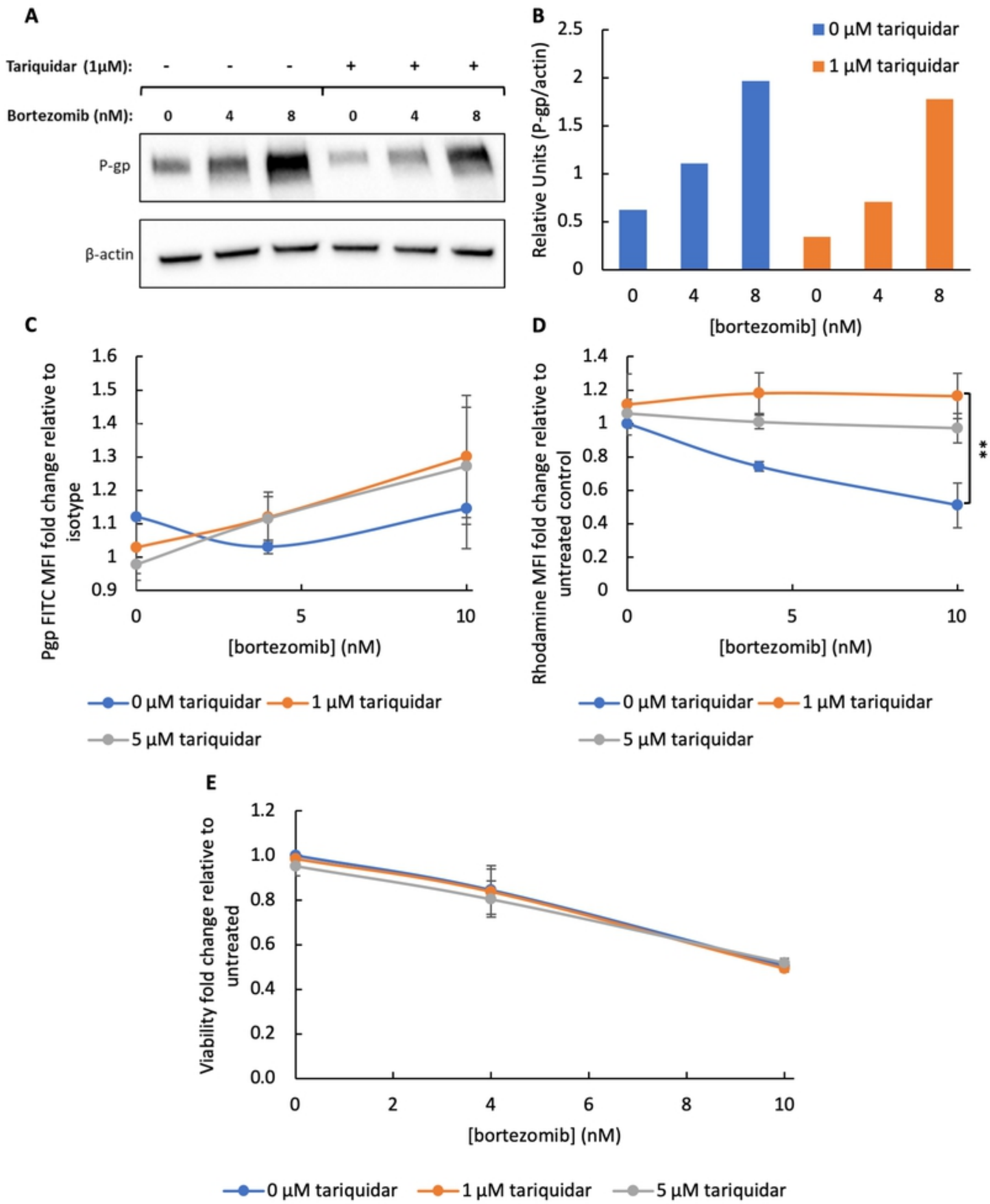
A
Tariquidar (1μM): - - - + + +
Bortezomib (nM): 0 4 8 0 4 8
P-gp
β-actin
B
0 μM tariquidar
1 μM tariquidar
Relative Units (P-gp/actin)
2.5
2
1.5
1
0.5
0
0 4 8 0 4 8
[bortezomib] (nM)
C
Pgp FITC MFI fold change relative to isotype
1.6
1.5
1.4
1.3
1.2
1.1
1
0.9
0 5 10
[bortezomib] (nM)
0 μM tariquidar
1 μM tariquidar
5 μM tariquidar
D
Rhodamine MFI fold change relative to untreated control
1.4
1.2
1
0.8
0.6
0.4
0.2
0
0 5 10
[bortezomib] (nM)
**
0 μM tariquidar
1 μM tariquidar
5 μM tariquidar
E
Viability fold change relative to untreated
1.2
1.0
0.8
0.6
0.4
0.2
0.0
0 2 4 6 8 10
[bortezomib] (nM)
0 μM tariquidar
1 μM tariquidar
5 μM tariquidar

Figure 4

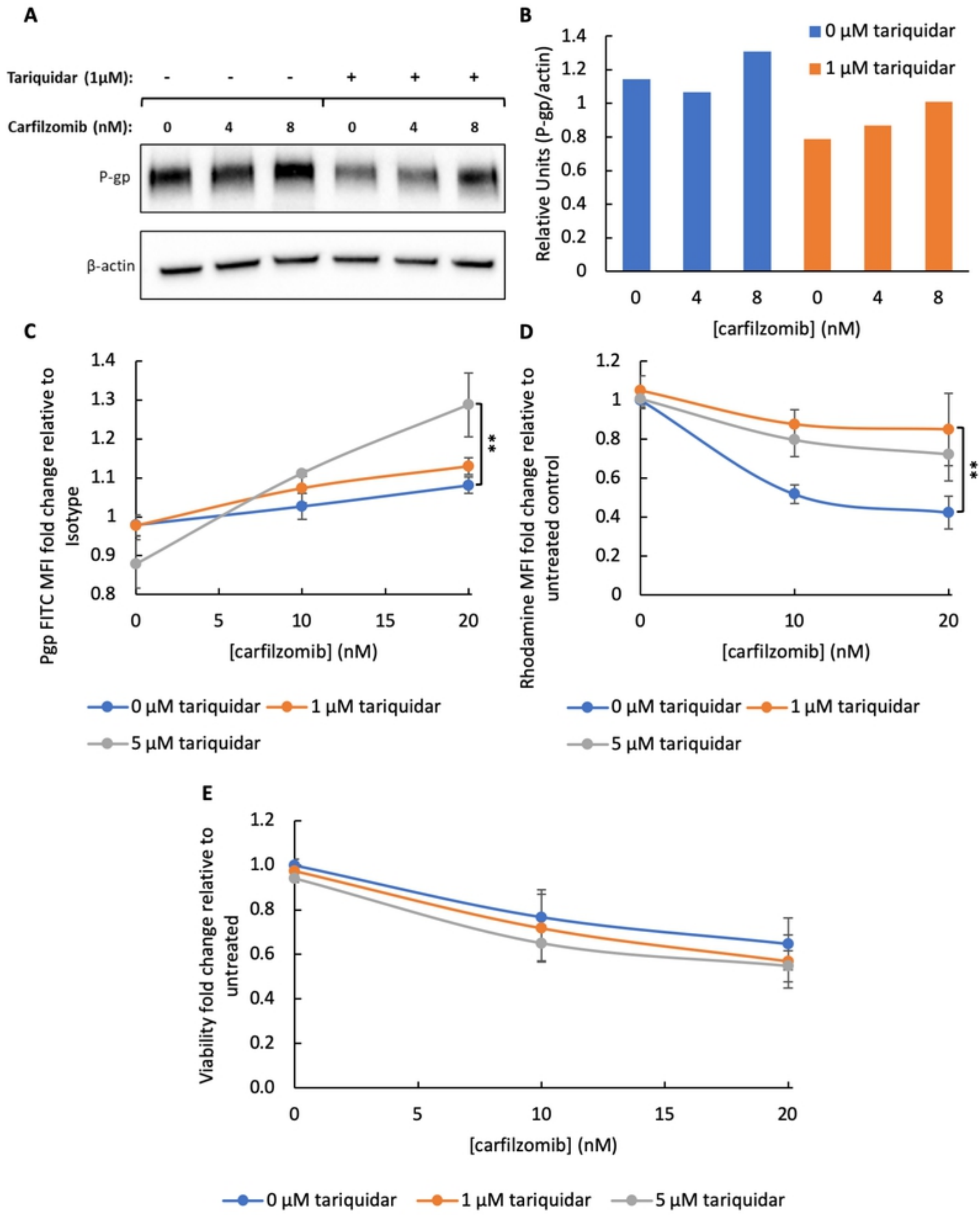
A
Tariquidar (1μM): - - - + + +
Carfilzomib (nM): 0 4 8 0 4 8
P-gp
β-actin
B
0 μM tariquidar
1 μM tariquidar
Relative Units (P-gp/actin)
1.4
1.2
1
0.8
0.6
0.4
0.2
0
0 4 8 0 4 8
[carfilzomib] (nM)
C
Pgp FITC MFI fold change relative to Isotype
1.4
1.3
1.2
1.1
1
0.9
0.8
**
0 5 10 15 20
[carfilzomib] (nM)
0 μM tariquidar
1 μM tariquidar
5 μM tariquidar
D
Rhodamine MFI fold change relative to untreated control
1.2
1
0.8
0.6
0.4
0.2
0
**
0 10 20
[carfilzomib] (nM)
0 μM tariquidar
1 μM tariquidar
5 μM tariquidar
E
Viability fold change relative to untreated
1.2
1.0
0.8
0.6
0.4
0.2
0.0
0 5 10 15 20
[carfilzomib] (nM)
0 μM tariquidar
1 μM tariquidar
5 μM tariquidar

Figure 5

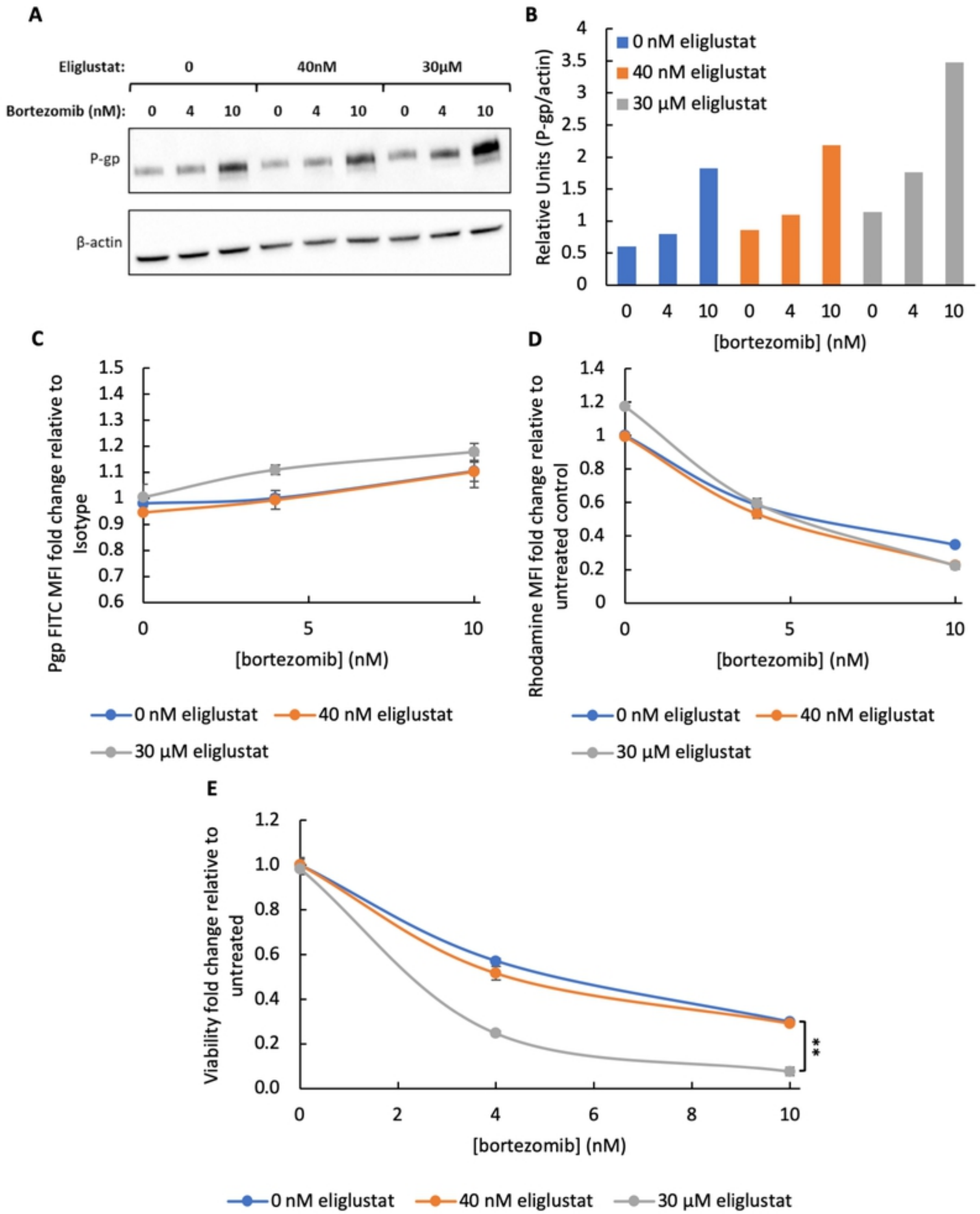
A
Eliglustat: 0 40nM 30μM
Bortezomib (nM): 0 4 10 0 4 10 0 4 10
P-gp
β-actin
B
0 nM eliglustat
40 nM eliglustat
30 μM eliglustat
Relative Units (P-gp/actin)
[bortezomib] (nM)
C
Pgp FITC MFI fold change relative to Isotype
[bortezomib] (nM)
0 nM eliglustat
40 nM eliglustat
30 μM eliglustat
D
Rhodamine MFI fold change relative to untreated control
[bortezomib] (nM)
0 nM eliglustat
40 nM eliglustat
30 μM eliglustat
E
Viability fold change relative to untreated
**
[bortezomib] (nM)
0 nM eliglustat
40 nM eliglustat
30 μM eliglustat

Figure 6

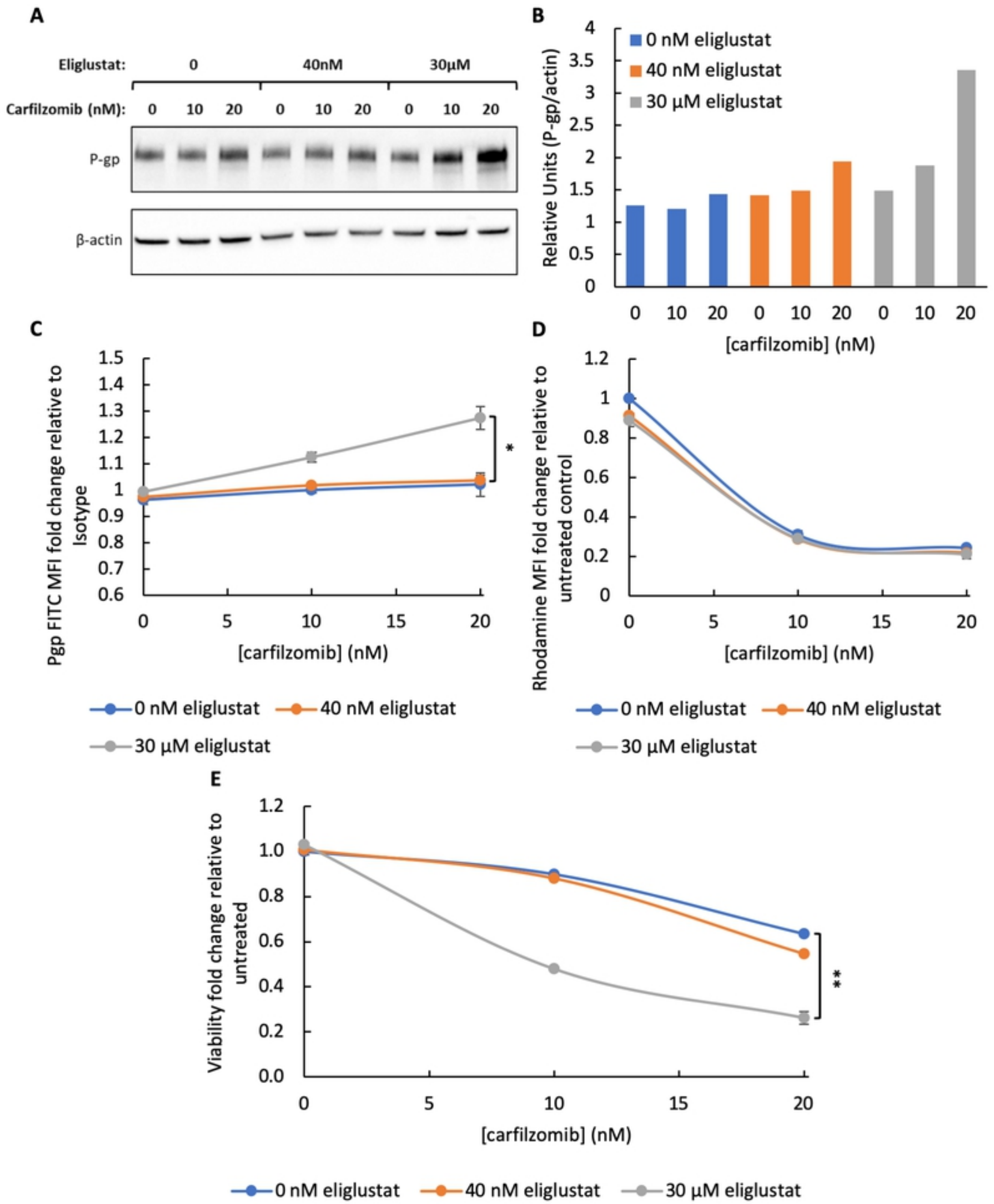
A
Eliglustat:
0
40nM
30µM
Carfilzomib (nM):
0 10 20 0 10 20 0 10 20
P-gp
β-actin
B
0 nM eliglustat
40 nM eliglustat
30 µM eliglustat
Relative Units (P-gp/actin)
[carfilzomib] (nM)
C
Pgp FITC MFI fold change relative to Isotype
[carfilzomib] (nM)
*
0 nM eliglustat
40 nM eliglustat
30 µM eliglustat
D
Rhodamine MFI fold change relative to untreated control
[carfilzomib] (nM)
0 nM eliglustat
40 nM eliglustat
30 µM eliglustat
E
Viability fold change relative to untreated
[carfilzomib] (nM)
**
0 nM eliglustat
40 nM eliglustat
30 µM eliglustat

Figure 7

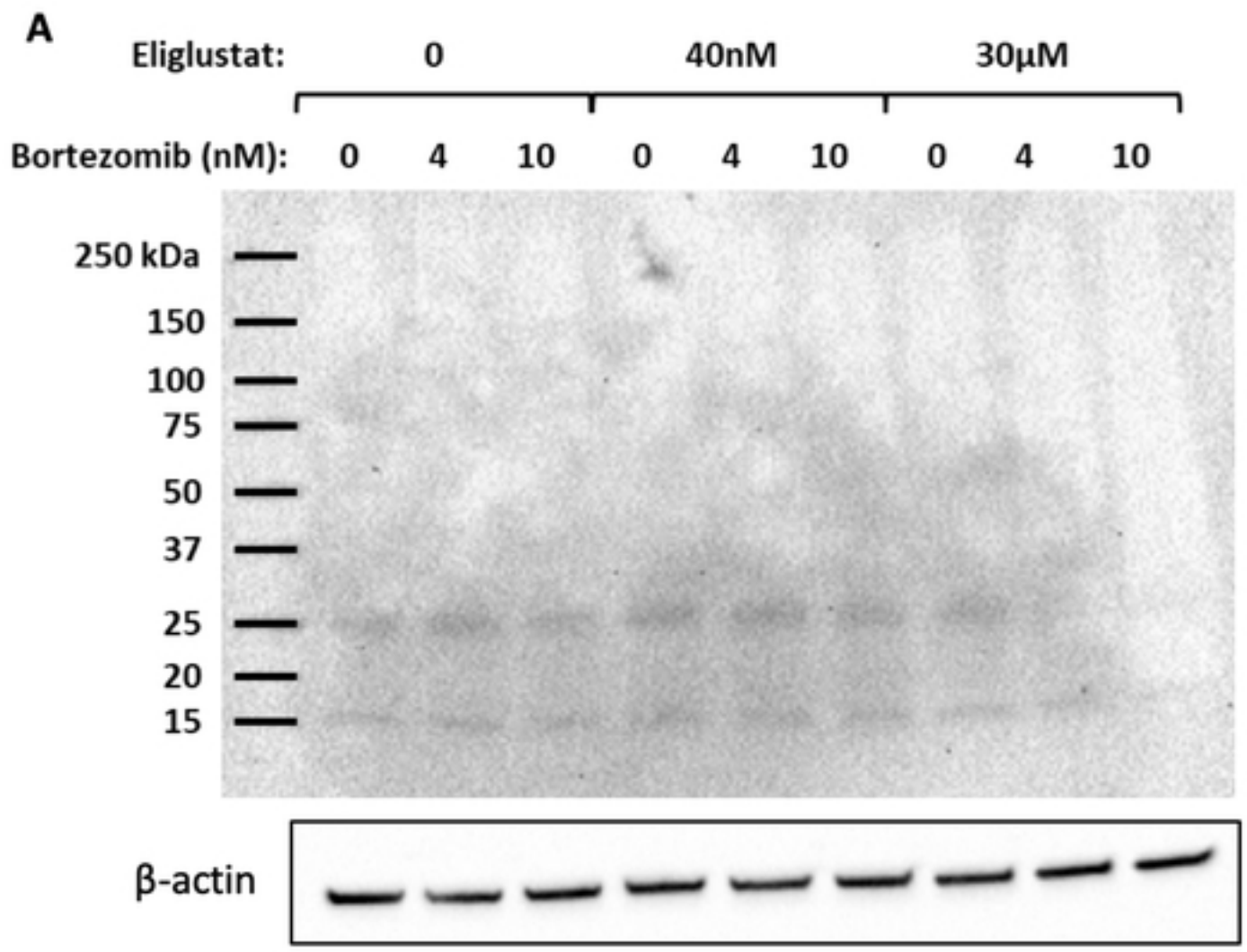
A
Eliglustat:
0
40nM
30µM
Bortezomib (nM):
0 4 10 0 4 10 0 4 10
250 kDa
150
100
75
50
37
25
20
15
β-actin

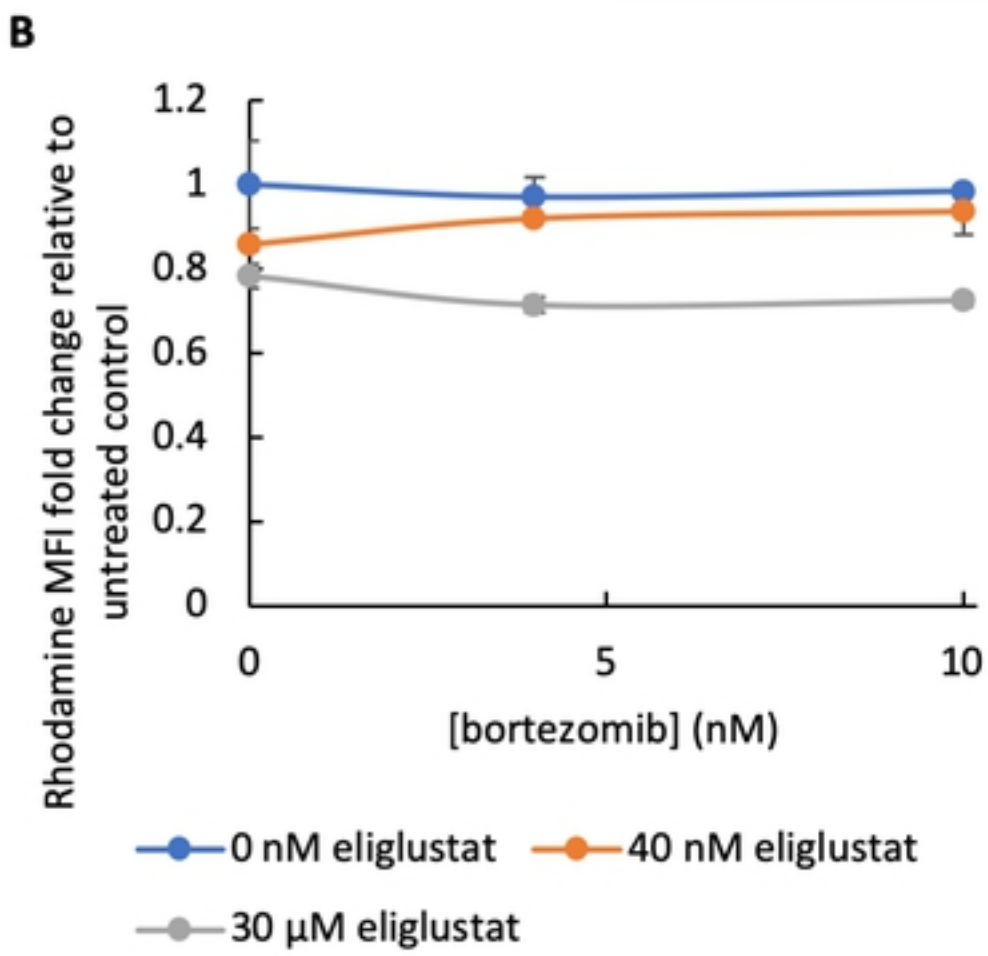
B
Rhodamine MFI fold change relative to untreated control
1.2
1
0.8
0.6
0.4
0.2
0
0
5
10
[bortezomib] (nM)
0 nM eliglustat
40 nM eliglustat
30 µM eliglustat

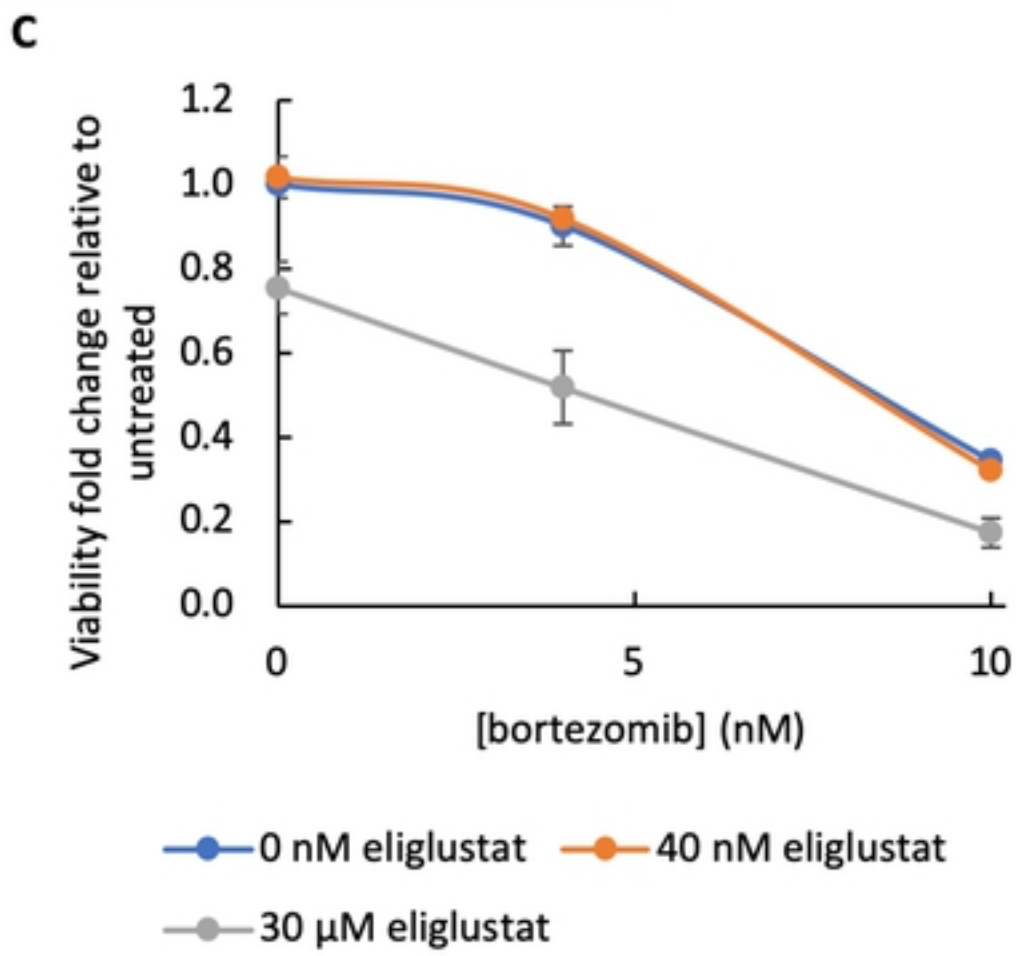
C
Viability fold change relative to untreated
1.2
1.0
0.8
0.6
0.4
0.2
0.0
0
5
10
[bortezomib] (nM)
0 nM eliglustat
40 nM eliglustat
30 µM eliglustat

Figure 8